JOURNAL OF VIROLOGY, Oct. 1999, p. 8732–8740 Vol. 73, No. 10
0022-538X/99/$04.00+0

Functional Analysis of the Interaction between VPg-Proteinase (NIa) and RNA Polymerase (NIb) of Tobacco Etch Potyvirus, Using Conditional and Suppressor Mutants

JOSÉ-ANTONIO DARÒS, MARY C. SCHAAD, AND JAMES C. CARRINGTON*

Institute of Biological Chemistry, Washington State University, Pullman, Washington 99164-6340

Received 20 April 1999/Accepted 8 July 1999

The tobacco etch potyvirus (TEV) RNA-dependent RNA polymerase (NIb) has been shown to interact with the proteinase domain of the VPg-proteinase (NIa). To investigate the significance of this interaction, a *Saccharomyces cerevisiae* two-hybrid assay was used to isolate conditional NIa mutant proteins with temperature-sensitive (*ts*) defects in interacting with NIb. Thirty-six unique *ts*NIa mutants with substitutions affecting the proteinase domain were recovered. Most of the mutants coded for proteins with little or no proteolytic activity at permissive and nonpermissive temperatures. However, three mutant proteins retained proteolytic activity at both temperatures and, in two cases (*ts*NIa-Q384P and *ts*NIa-N393D), the mutations responsible for the *ts* interaction phenotype could be mapped to single positions. One of the mutations (N393D) conferred a *ts*-genome-amplification phenotype when it was placed in a recombinant TEV strain. Suppressor NIb mutants that restored interaction with the *ts*NIa-N393D protein at the restrictive temperature were recovered by a two-hybrid selection system. Although most of the suppressor mutants failed to stimulate amplification of genomes encoding the *ts*NIa-N393D protein, two suppressors (NIb-I94T and NIb-C380R) stimulated amplification of virus containing the N393D substitution by approximately sevenfold. These results support the hypothesis that interaction between NIa and NIb is important during TEV genome replication.

Tobacco etch virus (TEV) is a member of the potyvirus family of positive-strand RNA viruses within the "picornavirus supergroup." The TEV genome (Fig. 1) consists of a 10-kb RNA molecule that is covalently linked to a virus-encoded protein (VPg) at its 5′ end (33). Genomic RNA encodes a single polyprotein that undergoes co- and posttranslational proteolytic processing. The processing events are catalyzed by three virus-encoded proteinases, termed P1, HC-Pro, and NIa (10).

Processing at most sites in the TEV polyprotein is catalyzed by the NIa proteinase, which resembles the 3C proteinase of picornaviruses (10). Most TEV NIa cleavage sites conform to a consensus heptapeptide motif containing four highly conserved positions: Glu-X-X-Tyr-X-Gln ↓ Gly/Ser (8). The conserved residues are necessary for efficient proteolysis and likely control the rates of processing in infected cells. Full-length NIa contains two domains, a C-terminal proteinase domain and an N-terminal VPg domain (9, 25, 36). A suboptimal NIa cleavage site separates the two domains, resulting in a mixture of full-length and internally cleaved forms of NIa (5, 9). Mutational analyses suggest that the slow processing feature at the internal cleavage site is required for TEV RNA replication (34). In addition, a second suboptimal cleavage site in NIa is located 24 residues from the C terminus within the proteinase domain (16, 27).

Most of the TEV-encoded proteins are needed directly or indirectly for genome replication. A set of core replication proteins catalyzes the essential enzymatic steps during RNA synthesis. These proteins include the CI helicase, the NIa VPg-proteinase, and the NIb RNA-dependent RNA polymerase (33). Replication complexes are associated with endoplasmic reticulum-derived membranes in infected cells (35). Association of replication complexes with membranes was proposed to involve the membrane-binding activity of the TEV 6-kDa protein (32, 35), which is positioned adjacent to the N terminus of NIa within the viral polyprotein. Further, it was proposed that the membrane-binding function of the 6-kDa protein is relevant within the context of a 6-kDa protein–NIa (6-NIa) polyprotein. Without the attachment of the 6-kDa protein, the NIa protein is transported efficiently to the nucleus (30, 31). The 6-NIa polyprotein, however, is retained in the cytoplasm on membrane surfaces. Release of the NIa protein from the 6-kDa protein occurs by autoproteolysis (4, 31).

Unlike NIa, the NIb polymerase appears not to be directed to replication complexes in the form of a membrane-binding polyprotein. Free NIb polymerase is functional within infected cells when it is produced independently of the TEV polyprotein (18, 20). Cellular transgenes encoding NIb polymerase can complement TEV genomes that lack a functional NIb coding sequence. Like NIa, however, free NIb polymerase can be targeted to the nucleus (19, 30). Direction of at least a subset of NIb polymerase molecules to replication complexes was proposed to involve protein-protein interactions with the membrane-bound 6-NIa polyprotein (20). Several studies have shown that potyviral NIb and NIa are able to interact specifically (11, 13, 20). Through deletion analysis, TEV NIb polymerase was shown to interact with the proteinase domain of NIa (20). In addition, an allele of NIb that lacks polymerase function but retains NIa-NIb interaction activity confers a dominant-negative phenotype (20), suggesting that the NIa-NIb interaction is important. Thus, two of the many steps in formation of TEV RNA replication complexes may be (i) binding of the 6-NIa polyprotein to endoplasmic reticulum-derived membranes and (ii) recruitment of NIb polymerase through protein-protein interaction with the proteinase domain of the membrane-bound polyprotein.

While the model described above is consistent with several

* Corresponding author. Mailing address: Institute of Biological Chemistry, Washington State University, Pullman, WA 99164-6340. Phone: (509) 335-2477. Fax: (509) 335-2482. E-mail: carrington@wsu.edu.

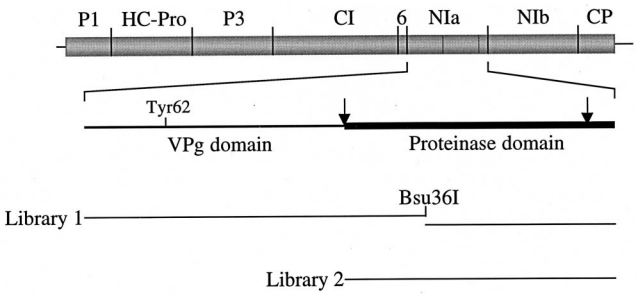

FIG. 1. Maps of the TEV genome, NIa, and sequences subjected to random mutagenesis. The TEV genome is represented at the top, with the polyprotein coding region indicated in grey. The names of several individual TEV proteins are given above the map. The sequences coding for cleavage sites are shown as short vertical lines within the coding region. The NIa sequence is represented in the expanded diagram, with the N-terminal VPg and C-terminal proteinase (thick line) domains indicated. Arrows indicate positions of suboptimal internal cleavage sites within NIa. The VPg attachment site (Tyr62) is indicated. The sequences independently mutagenized in the two libraries are shown at the bottom. Library 1 was composed of two sublibraries as represented by the two offset horizontal lines.

experimental observations, functional confirmation of the importance of these steps is lacking. In the present work, a genetic strategy was used to determine whether the NIa-NIb interaction is involved in TEV RNA replication. By a *Saccharomyces cerevisiae* two-hybrid system, temperature-sensitive (*ts*) NIa alleles with conditional NIa-NIb interaction defects were recovered and characterized. In addition, suppressor alleles of NIb that restored NIa-NIb interaction activity were produced and analyzed.

MATERIALS AND METHODS

Plasmids. Plasmid pTEV7DA-G ↓ H/KΔH contains a complete cDNA representing an infectious TEV-GUS genome (15). The GUS reporter gene is positioned between the P1 and HC-Pro coding regions (7). The NIa and NIb coding sequences were amplified by PCR from pTEV7DA-G ↓ H/KΔH with *Pfu* DNA polymerase. A stop codon was added after the last codon of each sequence. The NIa sequence was inserted between *Nco*I and *Xho*I sites of the activation domain plasmid pACT2 (Clontech), resulting in pACT-NIa. The NIb sequence was inserted between *Nde*I and *Sal*I sites of the DNA-binding-domain plasmid pAS2 (Clontech), resulting in pAS-NIb.

Site-directed mutagenesis. Site-specific mutations in NIa and NIb were generated by two consecutive PCRs. Mutations were introduced during the first reaction with a primer that contained the appropriate change. The product of the first reaction was purified and used as one of the primers in a second PCR. The product of the second reaction was cloned and sequenced. The PCR mixtures contained 10 mM Tris-HCl (pH 9.0), 50 mM KCl, 0.1% Triton X-100, 1.5 mM $MgCl_2$, 0.2 mM each deoxynucleoside triphosphate, 1 pmol of each PCR primer per μl, 0.05 U of *Pfu* DNA polymerase per μl, and 1 ng of template plasmid DNA per μl. Thirty reaction cycles were programmed for 40 s at 94°C, 30 s at 50°C, and 3 min at 72°C, preceded by an initial denaturation for 2 min at 94°C and followed by an extension for 10 min at 72°C.

Random mutagenesis. Randomly mutagenized sequences of NIa or NIb were generated by mutagenic PCR with pACT-NIa or pAS-NIb as the template, respectively. PCR conditions were as described above, but with the following changes. *Taq* DNA polymerase at 0.1 U/μl was used instead of *Pfu* DNA polymerase. For slightly mutagenic conditions, 0.1 mM $MnCl_2$ was included in the reaction mixture. For highly mutagenic conditions (3), 0.5 mM $MnCl_2$ was included and the concentrations of $MgCl_2$, dCTP, and dTTP were changed to 7, 1, and 1 mM, respectively.

Transformation of yeast. *S. cerevisiae* Y190 (MATa *gal4 gal80 his3 trp1-901 ade2-101 ura3-52 leu2,3-112/+ URA3*::*GAL* [*lacZ LYS2*::*GAL*] [*UAS*] [*HIS3 cyhR*]) and MaV103 (MATa *leu2-3,112 trp1-901 his3-200 ade2-101 gal4 gal80 SPAL10*::*URA3 GAL1*::*lacZ GAL1*::*HIS3@LYS2 can1R cyh2R*) (38) were used for the two-hybrid assays (12). Cells were transformed with supercoiled plasmid DNA by the lithium acetate method (2). Alternatively, yeast cells were transformed with a mix of PCR products and linearized vector DNA to allow gap repair reconstitution of plasmids in vivo (24).

Mutant protein selections and screens with the yeast two-hybrid system. Selections for yeast containing positive protein-protein interactors were done with synthetic complete medium (SC)-glucose plates containing 25 mM 3-amino-1,2,4-triazole but lacking Trp, Leu, and His or with SC-glucose plates lacking Trp, Leu, and uracil (2). Selections against yeast containing protein-protein interactors were done with SC-glucose plates containing 5-fluoroorotic acid (5-FOA; 0.1%) but lacking Trp and Leu.

Mutants with *ts* interaction defects in NIa were selected by one of two methods. For library 1, pACT-NIa plasmids containing mutagenized NIa sequences were introduced into yeast containing pAS-NIb. Transformed cells were selected for positive NIa-NIb interaction at the permissive temperature, 20°C. Colonies that grew were transferred to two fresh plates and selected for positive interaction at 20°C and at the nonpermissive temperature, 30°C. Those colonies that grew under selection at 20°C, but not at 30°C, contained candidate *ts*NIa mutants. For library 2, pACT-NIa plasmids containing mutagenized sequences were constructed by the in vivo gap repair transformation method in cells containing pAS-NIb. After selection for positive interactors at 20°C, colonies were transferred to replica plates containing two different media. One plate contained a medium selective for positive interaction and was incubated at 20°C. The other plate contained a counterselective medium with 5-FOA and was incubated at 30°C. Colonies that grew at 20 and 30°C were scored as candidate *ts* mutants.

All candidate *ts* mutants were also tested for protein-protein interaction at 20 and 30°C by a β-galactosidase filter assay with the colorimetric substrate 5-bromo-4-chloro-3-indolyl-β-D-galactopyranoside (X-Gal) (20). Mutagenized plasmids from all candidates that exhibited a *ts*-interaction phenotype in the β-galactosidase assay were recovered from the original yeast strains and tested for the *ts*-interaction phenotype after retransformation of yeast containing pAS-NIb. Only those mutants in which the *ts* phenotype was reproduced in the β-galactosidase plate assay with the retransformed strains were analyzed further. The NIa sequence in all mutagenized plasmids conferring a *ts*-interaction phenotype was sequenced.

Suppressor NIb mutant proteins that restored interaction with *ts*NIa-N393D at 30°C were recovered after random PCR mutagenesis (slightly mutagenic conditions) and selection in the yeast two-hybrid system. Colonies containing mutagenized pAS-NIb and pACT-tsNIa-N393D were recovered on a medium selective for positive interaction at 30°C. The pAS-NIb plasmids conferring a restored interaction phenotype were isolated, reintroduced into yeast containing pACT-tsNIa-N393D, and tested for interaction at 30°C by the β-galactosidase plate assay. The nucleotide sequences encoding all positively interacting NIb alleles were determined.

A quantitative β-galactosidase assay with liquid cultures of yeast containing each mutant plasmid was done. Cultures (1 ml) were grown to an optical density at 600 nm of 0.6 in SC-glucose medium lacking Trp and Leu. Cells were pelleted by centrifugation and resuspended in 1 ml of Z buffer (60 mM Na_2HPO_4, 40 mM NaH_2PO_4, 10 mM KCl, 1 mM $MgSO_4$, 50 mM β-mercaptoethanol [pH 7.0]). Ten microliters of 0.1% sodium dodecyl sulfate (SDS)–20 μl of chloroform was added to the suspension, and the mixture was vortexed vigorously. After addition of 0.2 ml of 4-mg/ml *o*-nitrophenyl-β-D-galactopyranoside (ONPG), the reaction mixture was incubated for 30 min at 30°C. The reaction was stopped by the addition of 0.5 ml of 1 M Na_2CO_3, and the cells were pelleted by centrifugation. The A_{420} of the supernatant was measured, and β-galactosidase activity units were calculated as described previously (22).

Proteolytic processing of NIa in *Escherichia coli*. Wild-type and mutant NIa coding sequences were transferred to the expression vector pET-23d(+) (Novagen) by using *Nco*I and *Xho*I restriction sites and introduced into *E. coli* BL21(DE3)pLysS (Novagen). Cells were grown to an optical density at 600 nm of 0.6, and expression was induced by addition of isopropyl-β-D-thiogalactopyranoside (IPTG) to a final concentration of 0.4 mM. Cultures were divided between two tubes and incubated at 20 and 30°C. Aliquots were withdrawn at different time points, and cells were pelleted by a brief centrifugation. Cells were resuspended in SDS-containing dissociation buffer in a final volume 1/10 of that of the original culture. Aliquots were incubated in a boiling-water bath for 5 min, followed by a 5-min centrifugation to remove insoluble material. Ten-microliter aliquots were subjected to SDS-polyacrylamide gel electrophoresis and immunoblot analysis with a cocktail of monoclonal antibodies directed against the NIa proteolytic domain (37).

Genome amplification assays in protoplasts. Mutations in NIa and NIb were introduced into plasmid pTEV7DA-G ↓ H/KΔH, which contains a full-length cDNA corresponding to a modified TEV genome (15). Capped RNA transcripts representing full-length TEV-GUS RNA were synthesized in vitro with SP6 RNA polymerase as described previously (7). Transcripts were concentrated by precipitation in 2 M LiCl and resuspended in deionized water. The concentration of transcripts in each experiment was normalized after quantitative densitometry. Approximately 10 μg of transcripts was used to inoculate *Nicotiana tabacum* cv. Xanthi nc protoplasts (7.5×10^5 cells per transfection) by the polyethylene glycol method (26). Protoplasts were harvested at 24, 48, and 72 h postinoculation (p.i.), and GUS activity was measured by a fluorometric assay (5). Activity was calculated as picomoles of the substrate 4-methylumbelliferyl glucuronide cleaved per minute per 10^5 protoplasts. In all experiments, each genome was tested in three replicate inoculations. Parental TEV-GUS and TEV-GUS/VNN (18) were used as positive and negative controls, respectively. In some experiments, relative amplification levels of mutants were calculated at the 48 or 72 h p.i. time point with either parental TEV-GUS or TEV-GUS/*ts*NIa-N393D as the standard.

TABLE 1. Summary of results of *ts*NIa mutant screens with the yeast two-hybrid system

Library	NIa sequence mutagenized	No. of mutagenized clones tested	No. of unique *ts*NIa mutants sequenced	No. of mutations/mutant (mean)	No. of proteinase-active mutants/no. of mutants tested[b]
1[a]	All	10^6	19	8.4	1/19
2	Proteinase domain	2×10^5	50	3.4	2/17

[a] Library 1 was composed of two sublibraries.
[b] Proteinase activity was tested by the NIa self-processing assay in *E. coli*.

RESULTS

NIa mutants with a *ts*-interaction phenotype. A random-mutagenesis strategy to isolate TEV NIa mutants with *ts* defects in the ability to interact with NIb polymerase was pursued with the yeast two-hybrid system. The two-hybrid system reproduces the NIa-NIb interaction efficiently and has been useful in mapping domains required for the interaction (20). *ts* mutants were sought for two reasons. First, the retention of NIa-NIb interaction activity at permissive temperatures ensures that each mutant has the potential to encode a viable protein. Second, *ts* mutants can be used to test the role of NIa-NIb interaction during TEV RNA replication. Two libraries of randomly mutagenized NIa sequences were created and screened for mutants that interacted with wild-type NIb at 20°C but not at 30°C. Interaction was tested by selection for growth and β-galactosidase assays.

The first library was generated under highly mutagenic PCR conditions. The NIa sequence (1,290 nucleotides) was independently mutagenized in two different segments, based only on the position of a convenient *Bsu*36I restriction site (nucleotide position 825) used for cloning. The first segment encompassed 64% of the NIa sequence, which coded for the VPg domain and approximately one-third of the proteinase domain (Fig. 1). The second segment coded for the remaining two-thirds of the proteinase domain. Each mutagenized population was inserted in place of the wild-type sequence in pACT-NIa. Approximately 10^6 *E. coli* transformants were obtained for each subpopulation (Table 1). Plasmid DNA was prepared in bulk and used to transform yeast cells containing pAS-NIb, after which colonies were grown under interaction-selective conditions at 20°C. Positive colonies were then tested for temperature sensitivity of interaction-dependent growth at 20 and 30°C. Isolates with a *ts*-growth phenotype under interaction-selective conditions were then screened for β-galactosidase activation with filter blots from colonies grown at 20 and 30°C (Fig. 2). A total of 35 *ts* mutants were recovered. Most of the mutants (31) were from the second sublibrary in which the 3′ end of the NIa coding sequence was mutagenized. Nucleotide sequence analysis revealed 19 unique alleles and 16 redundant alleles among the 35 original mutants (Table 1). Nearly all of the mutants contained multiple substitutions (8.4 per allele). Six of these contained mutations that introduced premature stop codons, resulting in truncations of between 5 and 25 residues from the C terminus of NIa.

A second library of randomly mutagenized NIa sequences was created, but with several differences relative to the first library. The mutagenic PCR conditions were modified to result in fewer substitutions. The mutagenesis target was restricted to the coding sequence for the proteinase domain (codons 189 to 430) (Fig. 1). Also, the gap repair method of transformation was used to clone the modified NIa alleles in pACT-NIa directly in yeast, thus bypassing the cloning step in *E. coli*. Finally, a yeast strain (MaV103) that incorporates a third reporter gene (*URA3*) for the two-hybrid system was used. Colonies were selected first for positive NIa-NIb interaction at 20°C. The colonies were then replica plated and subjected to a second round of selection at 30°C on a medium containing 5-FOA, which is converted to a toxic metabolite in the presence of active URA3. This selection eliminated colonies with positive NIa-NIb interactions at 30°C. The surviving colonies were replica plated and tested again for interaction activity at 20 and 30°C by selective growth and β-galactosidase assays. From a library of 2.5×10^5 yeast transformants containing mutagenized NIa sequences, 285 colonies exhibited a *ts* phenotype under interaction-selective conditions. The NIa sequence was determined in 52 of the pACT-NIa-derived plasmids, revealing 50 unique sequences with an average of 3.4 substitutions per allele (Table 1). Seven of the mutants contained substitutions that resulted in proteins with C-terminal truncations. Interestingly, 33 mutants contained a change in the codon for the carboxyl-terminal Gln (Q430) residue. Four of these contained a substitution resulting in Leu (Q430L), and 29 contained a substitution resulting in His (Q430H), although in all cases at least one additional mutation was present within the NIa proteinase domain coding sequence. However, introduction of neither the Q430L nor the Q430H mutation alone into an otherwise wild-type NIa sequence recreated the *ts* phenotype in NIa-NIb interaction assays (data not shown).

Proteolytic activities of *ts* NIa proteins. The NIb-interacting region of TEV NIa resides within the C-terminal proteolytic domain. To determine if the *ts*-interaction phenotypes were due to specific disruption of protein-protein interaction activity or to nonspecific disruption or misfolding of the proteinase domain, the proteolytic activities of the mutants were tested. The NIa coding regions from the mutants were transferred to the *E. coli* expression vector pET 23d(+). Cultures were

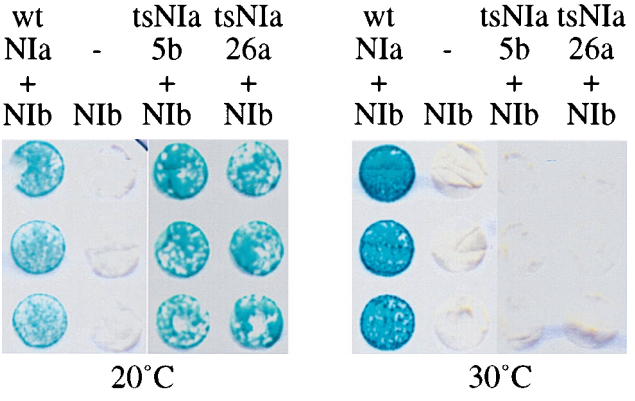

FIG. 2. Examples of β-galactosidase screens for temperature sensitivity of the NIa-NIb interaction in yeast. Colonies were plated in triplicate on each of two nitrocellulose filters incubated on interaction-nonselective medium, grown at 20 or 30°C, and processed for the β-galactosidase colorimetric assay. Results with two *ts*NIa mutant proteins (*ts*NIa-5b and *ts*NIa-26a) are shown along with those of positive-interaction and negative controls. wt, wild type.

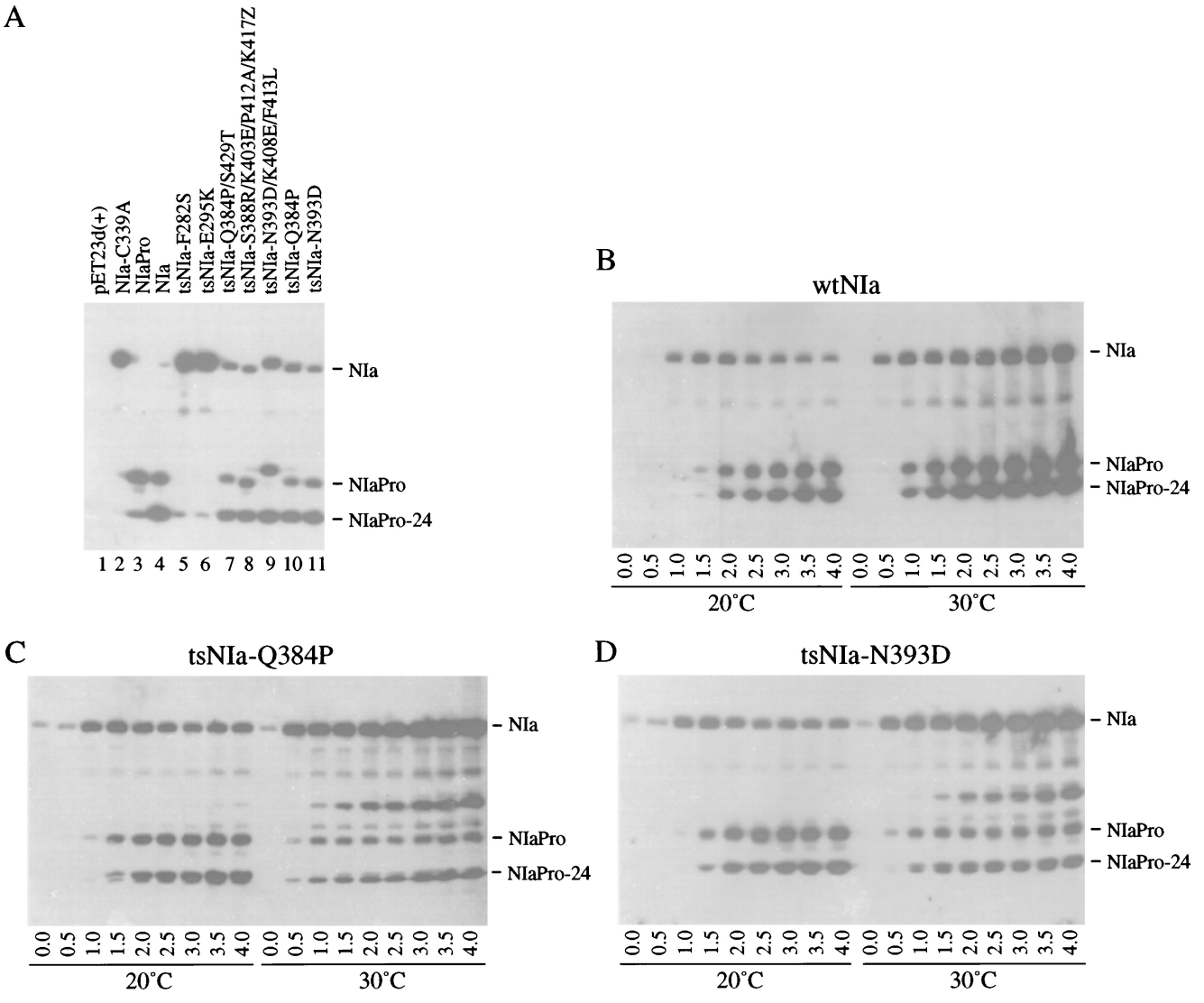

FIG. 3. Immunoblot assay for self-processing of selected *ts*NIa mutants in *E. coli*. (A) Cells were grown at 20°C, induced by addition of IPTG, cultured for an additional 4 h, and harvested. Total SDS-soluble protein extracts were subjected to immunoblot analysis with a monoclonal antibody cocktail specific for the proteinase domain of NIa. The cells contained an empty expression vector, pET23d(+), or a vector expressing the NIa-related protein indicated. (B to D) Time course analysis of self-processing at 20 and 30°C in *E. coli* with wild-type NIa (wtNIa) (B), *ts*NIa-Q384P (C), or *ts*NIa-N393D. Samples were withdrawn at the times postinduction (in hours) indicated below the gels and subjected to immunoblot assay with the antibody cocktail used in panel A. The positions of full-length NIa, the proteinase domain of NIa (NIaPro), and the proteinase domain lacking the C-terminal 24 residues (NIaPro-24) are shown next to each panel.

grown, expression was induced by addition of IPTG, and proteolytic function was assessed by an autoproteolytic cleavage assay (5, 34). The NIa protein undergoes self-cleavage at two positions after expression in *E. coli*: at a site between the VPg and proteinase domains and at a site 24 residues from the C terminus (Fig. 1). If cleavage occurs, immunoblot assay of extracts from induced cultures with monoclonal antibodies specific for the proteolytic domain would reveal the intact proteinase domain (NIaPro) and a truncated proteinase domain product (NIaPro-24), as well as any full-length NIa precursor that remains.

The proteolytic activities of the NIa's encoded by the 19 unique mutants from library 1 and the 17 mutants that encoded full-length NIa proteins with wild-type C-terminal residues from library 2 were tested first after cultures were grown at 20°C. As controls, wild-type NIa, a proteolytically inactive NIa mutant (NIa-C339A [4]) and NIaPro (6) were analyzed in parallel with the mutants. Expression of wild-type NIa resulted in the formation of NIaPro and NIaPro-24 cleavage products (Fig. 3A, lane 4). Expression of NIaPro also resulted in processing to yield NIaPro-24, although the majority of the protein remained intact (lane 3). In contrast, the defective NIa-C339A protein failed to process (lane 2). Among the *ts*NIa mutant proteins, only the *ts*NIa-Q384P/S429T (lane 7), *ts*NIa-S388R/K403E/P412A/K417Z (lane 8), and *ts*NIa-N393D/K408E/F413L (lane 9) proteins exhibited internal processing similar to that of wild-type NIa. Each of these mutant proteins contained at least two substitutions, and one (*ts*NIa-S388R/K403E/P412A/K417Z) contained a premature stop codon that shortened the protein by 13 residues. Each of these mutant proteins also self-processed at 30°C (data not shown). All other mutant proteins tested, as exemplified by *ts*NIa-F282S and

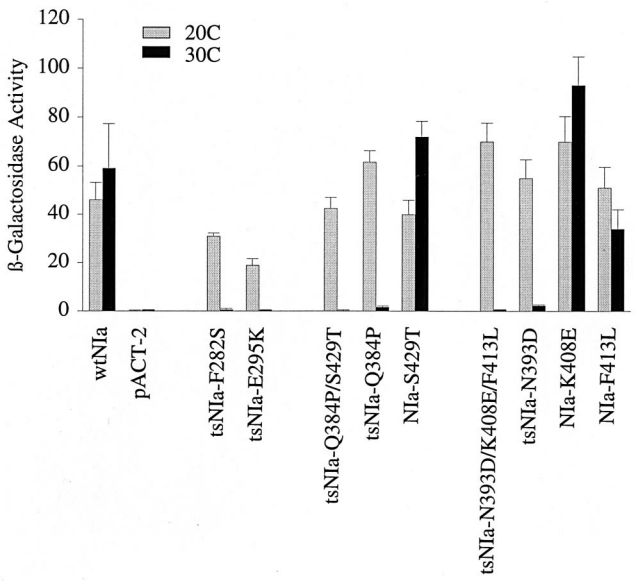

FIG. 4. Quantitative β-galactosidase assay for interaction in the yeast two-hybrid assay. Liquid cultures were grown in duplicate sets under interaction-nonselective conditions at 20 or 30°C. The yeast strains expressed the NIb fusion protein and empty cloning vector (pACT-2), wild-type NIa (wtNIa), or the mutant NIa's indicated. β-Galactosidase assays were done with three independent cultures for each strain at both temperatures, and the means ± standard deviations are plotted.

*ts*NIa-E295K, had either marginal or no proteolytic activity at 20°C (Fig. 3A, lanes 5 and 6; Table 1). Each of the *ts*NIa proteins that failed to process at 20°C also failed to process at 30°C (data not shown); most of these mutant proteins, therefore, were not characterized further.

Mapping *ts* mutations. As each of the three proteolytically active *ts*NIa mutants contained multiple substitutions, the effect of each individual mutation on NIa-NIb interaction in yeast was tested. Mutants containing single substitutions at the three alleles were constructed, and NIa-NIb interaction activity was inferred by quantitative β-galactosidase assays at 20 and 30°C. Parallel assays were done with strains expressing wild-type NIa, the three original proteolytically active *ts*NIa mutants, and two of the proteolytically inactive *ts*NIa mutants. Levels of interaction of wild-type NIa with NIb were similar at the two temperatures, whereas the interaction of each of the original mutant proteins with NIb was highly *ts* (Fig. 4). The Q384P mutation from the *ts*NIa-Q384P/S429T mutant protein conferred a *ts*-interaction phenotype, while the S429T mutation had little effect (Fig. 4). Similarly, only the N393D mutation from the *ts*NIa-N393D/K408E/F413L mutant protein conditioned a *ts*-interaction phenotype (Fig. 4). In contrast, each individual mutation from the *ts*NIa-S388R/K403E/P412A/K417Z mutant protein failed to recreate the *ts*-interaction phenotype (data not shown).

The single-substitution *ts*NIa-Q384P and *ts*NIa-N393D mutant proteins and wild-type NIa were analyzed for internal proteolytic processing activity in *E. coli* in time course accumulation assays at 20 and 30°C. At 120 to 150 min postinduction at 20°C, the amounts of wild-type precursor and products were roughly equivalent based on the intensities of the immunoblot signals (Fig. 3B). The time required for each of the mutant precursors and products to reach equivalent levels at 20°C was similar to that required for wild-type NIa (Fig. 3C and D), suggesting that the mutations had little effect on the efficiency of processing. At 30°C, both the wild-type NIa and mutant proteins accumulated to levels higher than at 20°C based on signal intensity. The wild-type and mutant proteins each underwent self-processing at 30°C, although the proportion of each protein that processed was lower than the proportion that processed at 20°C (Fig. 3B to D). The extent of self-processing of the mutant proteins over the time course was somewhat less than that of wild-type NIa at 30°C. Also, an additional proteolytic product with an electrophoretic mobility between those of full-length NIa and NIaPro was detected after induction of the mutant proteins, but not wild-type NIa, at 30°C. The basis for generation of this product, as well as the site of cleavage, was not investigated further.

Effects of *ts*NIa mutations on TEV genome amplification. The effect of the *ts*NIa-N393D and *ts*NIa-Q348P mutations on amplification of the viral genome was determined by a protoplast infection assay. In addition, two mutations (*ts*NIa-F282S and *ts*NIa-E295K) that conferred a *ts*-interaction phenotype but that severely affected proteolytic activity were tested. The mutations were introduced into the genome of TEV-GUS, a recombinant TEV strain that expresses the reporter protein β-glucuronidase. The parental TEV-GUS genome was used as the amplification-positive control, while the TEV-GUS/VNN genome, which contains a polymerase-inactivating mutation in the NIb coding sequence, was used as a negative control in all experiments. Transcripts corresponding to each genome were prepared in triplicate in all experiments and introduced into *N. tabacum* protoplasts. Cells in each inoculated culture were divided between two tubes for incubation at 20 or 30°C, and GUS activity was measured in samples taken at 24, 48, and 72 h p.i.

Parental TEV-GUS amplified with nearly linear kinetics between 24 and 72 h p.i. at both 20 and 30°C, although the absolute level of accumulation was higher at 20°C in all experiments (Fig. 5A). The TEV-GUS/*ts*NIa-N393D mutant exhibited a *ts*-amplification phenotype (Fig. 5A). In six independent experiments, TEV-GUS/*ts*NIa-N393D accumulated to 15% ± 6% (mean ± standard deviation) of the level of parental TEV-GUS at 20°C but to only 4% ± 3% at 30°C (Fig. 5B). The proteolytically active TEV-GUS/*ts*NIa-Q348P mutant, as well as the proteolytically defective TEV-GUS/*ts*NIa-F282S and TEV-GUS/*ts*NIa-E295K mutants, failed to amplify and was indistinguishable from the replication-defective TEV-GUS/VNN control at both temperatures (Fig. 5B).

NIb suppressor mutants that restore interaction with *ts*NIa-N393D. The *ts*NIa-N393D mutation conferred a *ts*-interaction phenotype with NIb and a *ts*-amplification phenotype in the context of the TEV-GUS genome. Although these results support the notion that the NIa-NIb interaction is necessary for efficient TEV amplification in infected cells, it is also possible that other NIa functions unrelated to NIa-NIb interaction activity were affected by the *ts*NIa-N393D substitution. To further investigate the basis for the *ts*-amplification defect conditioned by the *ts*NIa-N393D mutation, suppressor NIb mutants that restored interaction with *ts*NIa-N393D were isolated by the yeast two-hybrid assay and characterized. If the *ts*-amplification phenotype of the TEV-GUS/*ts*NIa-N393D mutant was due to the *ts*-interaction defect, then at least some NIb suppressor alleles would be expected to stimulate amplification in the presence of the *ts*NIa-N393D mutation.

A library of approximately 10^6 randomly mutagenized NIb sequences was generated by mutagenic PCR, and selections for interaction with *ts*NIa-N393D at 30°C were done to recover suppressor mutant candidates. Nineteen mutants were recovered, several of which restored two-hybrid interaction activity with *ts*NIa-N393D to levels comparable to those with wild-type

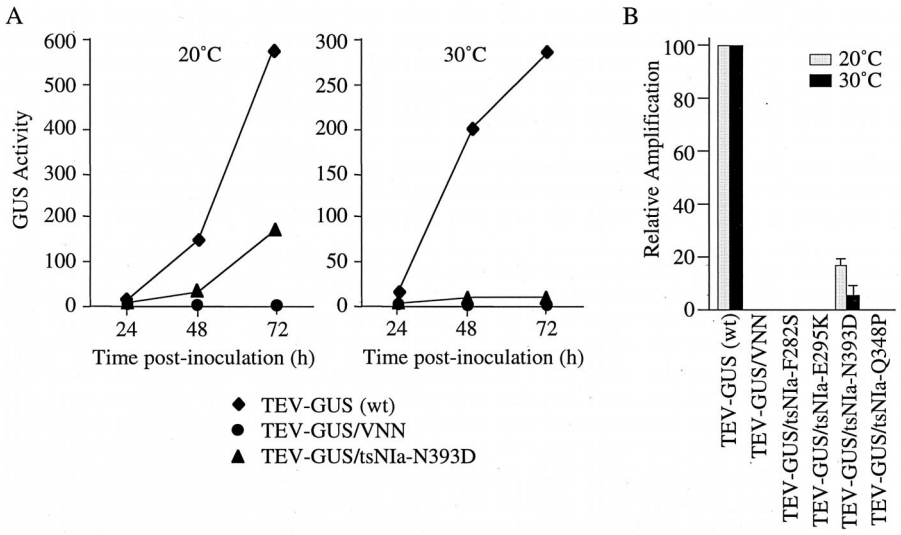

FIG. 5. Amplification of TEV-GUS genomes containing *ts*NIa mutant alleles in protoplasts. (A) Time course analysis of parental TEV-GUS, replication-defective TEV-GUS/VNN, and TEV-GUS/*ts*NIa-N393D at 20 and 30°C. Each data point represents the mean of results from three independent inoculations done simultaneously with the same batch of protoplasts. (B) Relative levels of amplification of control and *ts*NIa mutant TEV-GUS genomes in protoplasts at 20 and 30°C. Parental TEV-GUS (wild type [wt]) was used as the 100% standard at both temperatures. Each bar represents the mean relative amplification level (± standard deviation) at 48 h p.i. from six independent infections.

NIa and NIb sequences (Fig. 6A). Nucleotide sequence analysis of each mutant revealed 17 unique sequences with an average of 1.4 substitutions per mutant (Table 2). Five mutants contained either two or three substitutions, and in each case, at least one of the mutations also occurred in one of the single-substitution mutants. Three positions (M322, C380, and Y499) within NIb were affected by substitutions in multiple mutants (Table 2).

The NIb suppressor mutations in each of the single-substitution mutants, as well as the Y499N mutation from one of the multiple-substitution mutants, were transferred to the TEV-GUS/*ts*NIa-N393D mutant genome. Protoplasts were inoculated in triplicate and incubated at 30°C, and amplification was assessed by GUS activity assay at 72 h p.i. Amplification was calculated relative to that of the TEV-GUS/*ts*NIa-N393D mutant and plotted in Fig. 6B. As in other experiments, TEV-GUS with wild-type NIa and NIb sequences amplified to a level more than 20-fold greater than that of TEV-GUS/*ts*NIa-N393D. Most of the mutants with the NIb suppressor mutations amplified to levels similar to, or lower than, that of TEV-GUS/*ts*NIa-N393D. However, two NIb suppressor mutations, I94T and C380R, stimulated amplification to levels approximately sevenfold greater than that of TEV-GUS/*ts*NIa-N393D (Fig. 6B).

The TEV-GUS/*ts*NIa-N393D mutants with wild-type NIb, NIb-I94T, and NIb-C380R suppressor alleles were tested further in time course experiments with protoplasts at 20 and 30°C. At 20°C, the NIb-I94T and NIb-C380R alleles stimulated TEV-GUS/*ts*NIa-N393D amplification approximately twofold at 48 and 72 h p.i. (Fig. 7A). At 30°C, the suppressor mutations resulted in significantly greater relative levels of enhancement of TEV-GUS/*ts*NIa-N393D at each time point. At both temperatures, however, TEV-GUS/*ts*NIa-N393D with the NIb suppressor mutations amplified to levels of 50% or lower compared to the level of amplification of parental TEV-GUS (Fig. 7A). It was concluded that the NIb suppressor alleles conferred partial restoration of amplification activity to the TEV-GUS/*ts*NIa-N393D genome.

To determine if the NIb suppressors exhibited specificity for the *ts*NIa-N393D allele in the amplification assay, the wild-type NIa sequence was inserted into the TEV-GUS/*ts*NIa-N393D+NIb-I94T and TEV-GUS/*ts*NIa-N393D+NIb-C380R genomes in place of the mutant NIa sequence and genome amplification assays with protoplasts at 30°C were done. As in experiments described above, TEV-GUS/*ts*NIa-N393D genomes with the suppressor NIb mutations exhibited enhanced amplification activity relative to that of TEV-GUS/*ts*NIa-N393D with the wild-type NIb sequence but still significantly lower activity relative to that of parental TEV-GUS. The TEV-GUS genomes with suppressor NIb mutations and wild-type NIa sequences amplified to levels comparable to that of parental TEV-GUS, indicating that the suppressor NIb proteins did not possess unique compatibilities with the *ts*NIa-N393D protein for replicative functions. These results also suggest that the basis for enhanced amplification of the TEV-GUS/*ts*NIa-N393D mutants with suppressor NIb alleles was not due simply to inherently elevated polymerase activities of the suppressor NIb proteins but rather to the enhanced NIa-NIb interaction.

DISCUSSION

The yeast two-hybrid system proved to be useful for isolation of NIa-NIb *ts*-interaction mutants, as well as suppressor mutants with restored interaction activities. As with a number of other examples, the ability to modulate the protein-protein interaction phenotype in the yeast system provided tools to allow assessment of the functional significance of the interaction in infected cells (39). A similar strategy was used successfully by Hope et al. (14) to isolate *ts* mutants of poliovirus 3D with defects in interaction with 3AB protein.

As predicted from previous deletion analyses (20), most or all of the *ts*NIa mutants contained substitutions affecting the proteinase domain. However, over 90% of the 36 *ts*NIa mutants tested lost most or all proteolytic activity at both the interaction-permissive and -nonpermissive temperatures. The proteinase-defective mutants, therefore, had substitutions that resulted in temperature-independent structural perturbations or misfolding defects that clearly affected more than simply

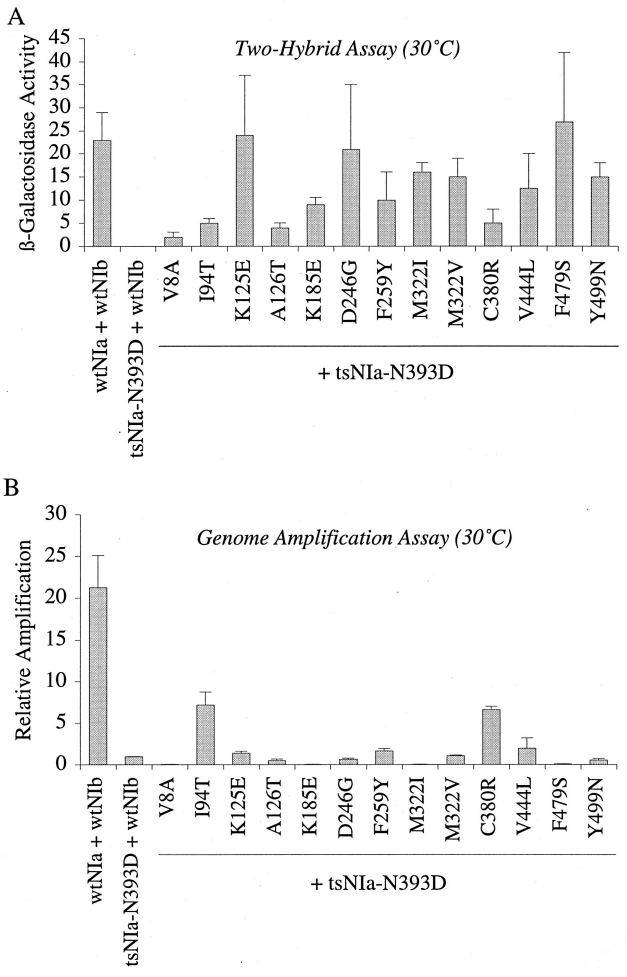

FIG. 6. Isolation and analysis of NIb suppressor mutant proteins that restore interaction with *ts*NIa-N393D at 30°C in the yeast two-hybrid system. (A) Quantitative β-galactosidase assays of yeast cultures containing pACT-tsNIa-N393D and pAS-NIb alleles with the indicated mutations. Each bar represents the mean activity (± standard deviation) (in Miller units) from three independent cultures. (B) Relative levels of stimulation of amplification of TEV-GUS/*ts*NIa-N393D genomes containing the NIb suppressor alleles indicated in protoplasts at 48 h p.i. Amplification was calculated by using TEV-GUS/*ts*NIa-N393D, with results for wild-type NIb (wtNIb) as the relative standard being equal to 1. Each bar represents the mean (± standard deviation) of results from three independent infections.

TABLE 2. Unique suppressor mutants found in an NIb suppressor mutant screen[a]

Unique suppressor mutant (n = 17)
NIb-V8A
NIb-I94T
NIb-K125E
NIb-A126T
NIb-K185E
NIb-D246G
NIb-F259Y
NIb-M322I
NIb-M322V
NIb-C380R
NIb-V444L
NIb-F479S
NIb-V85M-M322I
NIb-C380S-T487S
NIb-K185E-K421E-F479S
NIb-A121T-D248G-Y499N
NIb-K333R-N346H-Y499N

[a] The entire NIb sequence was mutagenized, and 10^6 clones were tested. The total number of suppressor mutants isolated was 19, and the mean number of mutations per mutant was 1.4.

protein-protein interaction. As NIa proteinase-defective mutants of TEV fail to replicate, this large class of mutants was not particularly valuable. The finding of three proteinase-active, *ts*-interaction-defective mutants, on the other hand, indicated that NIa-NIb interaction and proteinase activities could be separated genetically. These mutants likely had subtle defects without significant disruption of protein structure, at least at 20°C. The two mutations (Q384P and N393D) that could be mapped to single positions were predicted to affect a region of the proteinase that is beyond the sequence of relatively high similarity with the picornavirus 3C proteinases (data not shown). As a result, the homologous sites within the three-dimensional structure of the 3C proteinase (1, 21) could not be ascertained.

Although the *ts*NIa-Q384P and *ts*NIa-N393D mutants exhibited comparable interaction defects in the two-hybrid system and similar self-processing characteristics in *E. coli*, they were distinguishable by their effects on genome amplification in inoculated protoplasts. Whereas the TEV-GUS/*ts*NIa-N393D mutant displayed a *ts*-amplification defect, the TEV-GUS/*ts*NIa-Q394P mutant was nonviable at the two temperatures tested. The basis for this difference is not immediately clear. It is possible that an NIa function distinct from interaction with NIb or proteolytic activity, such as RNA-binding activity (6), was affected by the *ts*NIa-Q384P mutation. Alternatively, significant deviations from the protein-protein interaction or proteolytic activities detected in the experimental assay systems may have occurred in the context of infected cells. For example, the *ts*NIa-Q384P mutation may have had a more detrimental impact on NIa proteolytic activity in infected cells than it did on self-processing in *E. coli*. It should be noted that self-processing of both *ts*NIa-Q384P and *ts*NIa-N393D in *E. coli* resulted in formation of a spurious cleavage product, the consequence of which is not known.

The *ts*NIa-N393D mutation was most interesting, as it conferred *ts*-NIa-NIb-interaction and *ts*-amplification phenotypes. The most straightforward interpretation of these results is that the *ts*-amplification phenotype was due to the NIa-NIb interaction defect. However, there are also other explanations, such as the possibility that both the conditional interaction and the amplification defects were due to *ts* folding or protein destabilization effects. The observation of an additional self-proteolytic product and lower level of proteolytic activity than that of wild-type NIa at 30°C leaves open the possibility that *ts*NIa-N393D protein was structurally compromised.

The NIb suppressor mutant strategy was designed to shed light on the basis for the *ts*-amplification defect caused by the *ts*NIa-N393D mutations. If the amplification defect was due specifically to NIa-NIb interaction defects, then at least some of the interaction restoration suppressor mutants of NIb from the yeast two-hybrid system should have stimulated amplification of genomes containing the *ts*NIa-N393D mutation. If the amplification defect was due to reasons other than the NIa-NIb interaction activity, then none of the NIb suppressor mutations were predicted to have any positive effect on amplification of the *ts*NIa-N393D mutant genomes. The suppressor mutant strategy was considered ideal for analyzing the basis for the NIa defect, especially in view of the multifunctionality of the

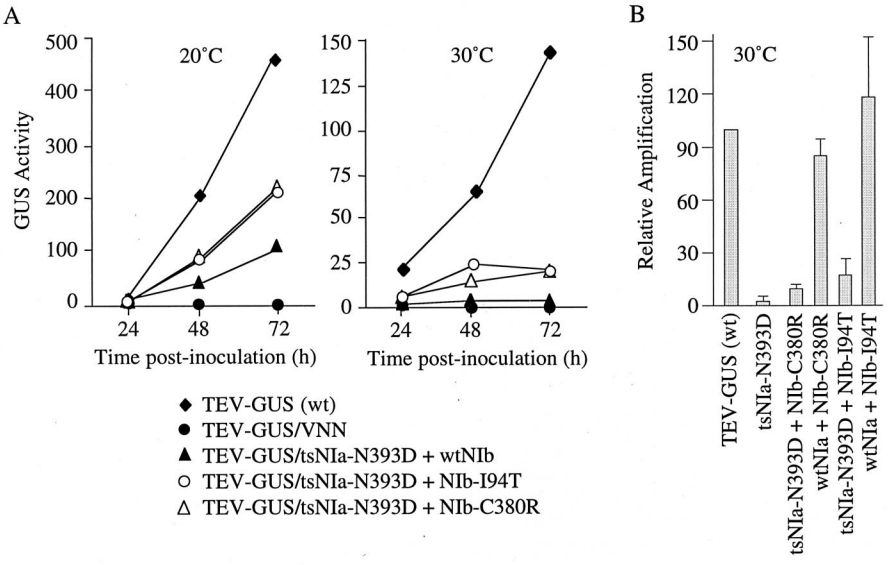

FIG. 7. Amplification of TEV-GUS/*ts*NIa-N393D mutant genomes containing NIb suppressor alleles in protoplasts. (A) Time course analysis of parental TEV-GUS (wild type [wt]), replication-defective TEV-GUS/VNN, and TEV-GUS/*ts*NIa-N393D with the wild-type NIb, NIb-I94T, or NIb-C380R allele at 20 and 30°C. Each data point represents the mean of results from three independent inoculations done simultaneously with the same batch of protoplasts. (B) Relative levels of amplification of TEV-GUS mutant genomes containing the NIb suppresor alleles with wild-type NIa or the *ts*NIa-N393D allele in protoplasts at 30°C. Parental TEV-GUS was used as the 100% standard. Each bar represents the mean relative amplification level (± standard deviation) at 48 h p.i. from three independent infections.

NIa protein and the difficulty in discerning all of the consequences of any given mutation. A potential flaw in this strategy was the possibility of introduction of mutations with deleterious effects on NIb polymerase activity, irrespective of the gain-of-interaction phenotype; indeed, several mutants with this characteristic were recovered. However, two of the 17 NIb suppressor alleles analyzed stimulated amplification of the TEV-GUS/*ts*NIa-N393D mutant genome, although not to levels equivalent to that of parental virus lacking any mutations. The amplification enhancement provided by the suppressor mutations occurred at both low and high temperatures. Further, the amplification-enhancing phenotype conferred by the NIb suppressor mutations was not explained by a generally increased activity of the NIb polymerase, as the suppressor alleles in a genomic context containing wild-type NIa conditioned amplification activity to levels similar to that of the wild-type NIb allele. The fact that amplification-enhancing suppressor mutations were recovered from the two-hybrid screen points strongly to the conclusion that the *ts*NIa-N393D mutation conferred an amplification-defective phenotype that was at least partly due to NIa-NIb interaction defects.

While the functional analysis described here supports the idea of NIa-NIb interaction serving an important role during TEV RNA replication, it does not pinpoint the step at which this interaction occurs. It has been hypothesized that free NIb polymerase is recruited to membrane-bound initiation sites through interaction with the proteinase domain of the 6-NIa polyprotein (6, 20, 35). Interaction of NIb with the proteinase domain of NIa would then result in positioning of the polymerase adjacent to the VPg domain for stimulation of polymerase activity and protein priming of RNA synthesis. Fellers et al. (11) showed that interaction of NIb with either NIa or the VPg domain stimulates NIb polymerase activity in vitro, although the stimulation appears to occur through a protein-priming-independent mechanism. These steps may be functionally analogous to the protein-protein interaction postulated to occur during initiation of picornavirus RNA synthesis, where 3D polymerase interacts with the membrane-bound VPg precursor 3AB (14, 23). Interaction of 3AB with 3D also stimulates the polymerase activity of 3D in vitro (17, 28, 29). Therefore, the interaction of NIa with NIb may represent a highly conserved core feature of the RNA replication apparatus of viruses within the picornavirus supergroup.

ACKNOWLEDGMENTS

We are grateful to M. Vidal for supplying us with the counterselectable yeast two-hybrid system.

This work was supported by a grant from the National Institutes of Health (AI27832) to J.C.C. and by a fellowship from the Ministry of Education and Science in Spain to J.-A.D.

REFERENCES

1. **Allaire, M., M. M. Chernaia, B. A. Malcolm, and M. N. James.** 1994. Picornaviral 3C cysteine proteinases have a fold similar to chymotrypsin-like serine proteinases. Nature **369:**72–76.
2. **Ausubel, F., R. Brent, R. E. Kingston, D. D. Moore, J. G. Seidman, J. A. Smith, and K. Struhl (ed.).** 1995. Short protocols in molecular biology, 3rd ed. John Wiley and Sons, Inc., New York, N.Y.
3. **Cadwell, R., and G. Joyce.** 1992. Randomization of genes by PCR mutagenesis. PCR Methods Appl. **2:**28–33.
4. **Carrington, J. C., and W. G. Dougherty.** 1987. Processing of the tobacco etch virus 49K protease requires autoproteolysis. Virology **160:**355–362.
5. **Carrington, J. C., R. Haldeman, V. V. Dolja, and M. A. Restrepo-Hartwig.** 1993. Internal cleavage and *trans*-proteolytic activities of the VPg-proteinase (NIa) of tobacco etch potyvirus in vivo. J. Virol. **67:**6995–7000.
6. **Daròs, J. A., and J. C. Carrington.** 1997. RNA-binding activity of NIa proteinase of tobacco etch potyvirus. Virology **237:**327–336.
7. **Dolja, V. V., H. J. McBride, and J. C. Carrington.** 1992. Tagging of plant potyvirus replication and movement by insertion of β-glucuronidase into the viral polyprotein. Proc. Natl. Acad. Sci. USA **89:**10208–10212.
8. **Dougherty, W. G., S. M. Cary, and T. D. Parks.** 1989. Molecular genetic analysis of a plant virus polyprotein cleavage site: a model. Virology **171:** 356–364.
9. **Dougherty, W. G., and T. D. Parks.** 1991. Post-translational processing of the tobacco etch virus 49-kDa small nuclear inclusion polyprotein: identification of an internal cleavage site and delimitation of VPg and proteinase domains. Virology **183:**449–456.
10. **Dougherty, W. G., and B. L. Semler.** 1993. Expression of virus-encoded proteinases: functional and structural similarities with cellular enzymes. Microbiol. Rev. **57:**781–822.

11. **Fellers, J., J. Wan, Y. Hong, G. B. Collins, and A. G. Hunt.** 1998. In vitro interactions between a potyvirus-encoded, genome-linked protein and RNA-dependent RNA polymerase. J. Gen. Virol. **79:**2043–2049.
12. **Fields, S., and O. K. Song.** 1989. A novel genetic system to detect protein-protein interactions. Nature **340:**245–246.
13. **Hong, Y., K. Levay, J. F. Murphy, P. G. Klein, J. G. Shaw, and A. G. Hunt.** 1995. The potyvirus polymerase interacts with the viral coat protein and VPg in yeast cells. Virology **214:**159–166.
14. **Hope, D. A., S. E. Diamond, and K. Kirkegaard.** 1997. Genetic dissection of interaction between poliovirus 3D polymerase and viral protein 3AB. J. Virol. **71:**9490–9498.
15. **Kasschau, K. D., and J. C. Carrington.** 1995. Requirement for HC-Pro processing during genome amplification of tobacco etch potyvirus. Virology **209:**268–273.
16. **Kim, D. H., Y. S. Park, S. S. Kim, J. Lew, H. G. Nam, and K. Y. Choi.** 1995. Expression, purification, and identification of a novel self-cleavage site of the NIa C-terminal 27-kDa protease of turnip mosaic potyvirus C5. Virology **213:**517–525.
17. **Lama, J., M. A. Sanz, and P. L. Rodriguez.** 1995. A role for 3AB protein in poliovirus genome replication. J. Biol. Chem. **270:**14430–14438.
18. **Li, X. H., and J. C. Carrington.** 1995. Complementation of tobacco etch potyvirus mutants by active RNA polymerase expressed in transgenic cells. Proc. Natl. Acad. Sci. USA **92:**457–461.
19. **Li, X. H., and J. C. Carrington.** 1993. Nuclear transport of tobacco etch potyviral RNA-dependent RNA polymerase is highly sensitive to sequence alterations. Virology **193:**951–958.
20. **Li, X. H., P. Valdez, R. E. Olvera, and J. C. Carrington.** 1997. Functions of the tobacco etch virus RNA polymerase (NIb): subcellular transport and protein-protein interaction with VPg/proteinase (NIa). J. Virol. **71:**1598–1607.
21. **Matthews, D. A., W. W. Smith, R. A. Ferre, B. Condon, G. Budahazi, W. Sisson, J. E. Villafranca, C. A. Janson, H. E. McElroy, C. L. Gribskov, and S. Worland.** 1994. Structure of human rhinovirus 3C protease reveals a trypsin-like polypeptide fold, RNA-binding site, and a means for cleaving precursor polyprotein. Cell **77:**761–771.
22. **Miller, J. H.** 1972. Experiments in molecular genetics. Cold Spring Harbor Laboratory, Cold Spring Harbor, N.Y.
23. **Molla, A., K. S. Harris, A. V. Paul, S. H. Shin, J. Mugavero, and E. Wimmer.** 1994. Stimulation of poliovirus proteinase $3CP^{ro}$-related proteolysis by the genome-linked protein VPg and its precursor 3AB. J. Biol. Chem. **269:**27015–27020.
24. **Muhlrad, D., R. Hunter, and R. Parker.** 1992. A rapid method for localized mutagenesis of yeast genes. Yeast **8:**79–82.
25. **Murphy, J. F., R. E. Rhoads, A. G. Hunt, and J. G. Shaw.** 1990. The VPg of tobacco etch virus RNA is the 49 kDa proteinase or the N-terminal 24 kDa part of the proteinase. Virology **178:**285–288.
26. **Negrutiu, I., R. Shillito, I. Potrykus, G. Biasini, and F. Sala.** 1987. Hybrid genes in the analysis of transformation conditions. 1. Setting up a simple method for direct gene transfer in plant protoplasts. Plant Mol. Biol. **8:**363–373.
27. **Parks, T. D., E. D. Howard, T. J. Wolpert, D. J. Arp, and W. G. Dougherty.** 1995. Expression and purification of a recombinant tobacco etch virus NIa proteinase: biochemical analysis of the full-length and a naturally occurring truncated proteinase form. Virology **210:**194–201.
28. **Paul, A. V., X. Cao, K. S. Harris, J. Lama, and E. Wimmer.** 1994. Studies with poliovirus polymerase $3D^{pol}$: stimulation of poly(U) synthesis in vitro by purified poliovirus protein 3AB. J. Biol. Chem. **269:**29173–29181.
29. **Plotch, S. J., and O. Palant.** 1995. Poliovirus protein 3AB forms a complex with and stimulates the activity of the viral RNA polymerase, $3D^{pol}$. J. Virol. **69:**7169–7179.
30. **Restrepo, M. A., D. D. Freed, and J. C. Carrington.** 1990. Nuclear transport of plant potyviral proteins. Plant Cell **2:**987–998.
31. **Restrepo-Hartwig, M. A., and J. C. Carrington.** 1992. Regulation of nuclear transport of a plant potyvirus protein by autoproteolysis. J. Virol. **66:**5662–5666.
32. **Restrepo-Hartwig, M. A., and J. C. Carrington.** 1994. The tobacco etch potyvirus 6-kilodalton protein is membrane associated and involved in viral replication. J. Virol. **68:**2388–2397.
33. **Riechmann, J. L., S. Laín, and J. A. García.** 1992. Highlights and prospects of potyvirus molecular biology. J. Gen. Virol. **73:**1–16.
34. **Schaad, M. C., R. Haldeman-Cahill, S. Cronin, and J. C. Carrington.** 1996. Analysis of the VPg-proteinase (NIa) encoded by tobacco etch potyvirus: effects of mutations on subcellular transport, proteolytic processing and genome amplification. J. Virol. **70:**7039–7048.
35. **Schaad, M. C., P. Jensen, and J. C. Carrington.** 1997. Formation of plant RNA virus replication complexes on membranes: role of an endoplasmic reticulum-targeted viral protein. EMBO J. **16:**4049–4059.
36. **Shahabuddin, M., J. G. Shaw, and R. E. Rhoads.** 1988. Mapping of the tobacco vein mottling virus VPg cistron. Virology **163:**635–637.
37. **Slade, D. E., R. E. Johnston, and W. G. Dougherty.** 1989. Generation and characterization of monoclonal antibodies reactive with the 49-kDa proteinase of tobacco etch virus. Virology **173:**499–508.
38. **Vidal, M., R. K. Brachmann, A. Fattaey, E. Harlow, and J. D. Boeke.** 1996. Reverse two-hybrid and one-hybrid systems to detect dissociation of protein-protein and DNA-protein interactions. Proc. Natl. Acad. Sci. USA **93:**10315–10320.
39. **Vidal, M., and P. Legrain.** 1999. Yeast forward and reverse 'n'-hybrid systems. Nucleic Acids Res. **27:**919–929.